



STRUCTURAL
CHEMISTRY

Volume 76 (2020)

Supporting information for article:

Temperature-induced solid-to-solid transformation in helical homochiral coordination polymers

Zhong-Xuan Xu, Guo-Guo Chen and Li-Feng Li

Table S1. Some selected bond lengths (\AA) and bond angles ($^\circ$) in **1-L**, **1-D**, **2-L** and **2-D**

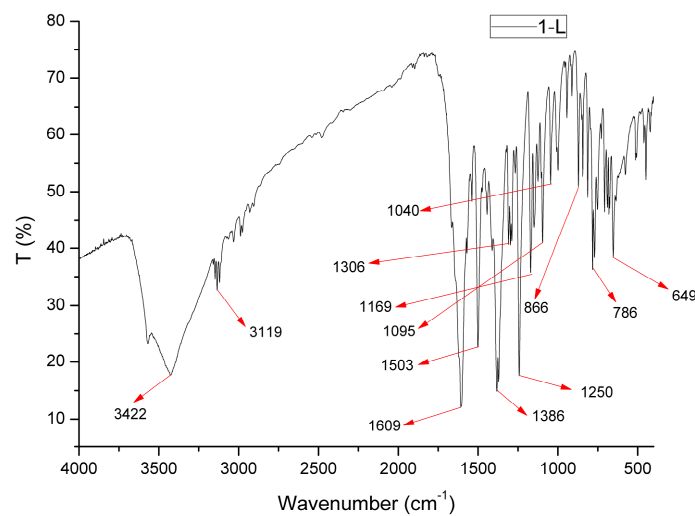
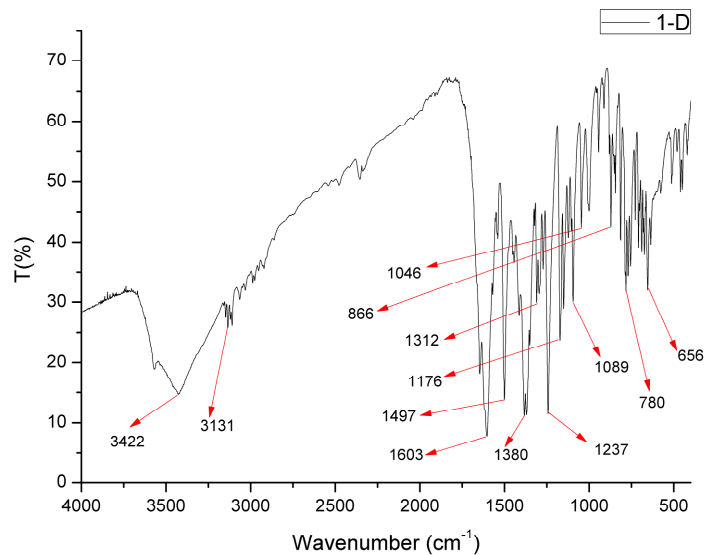
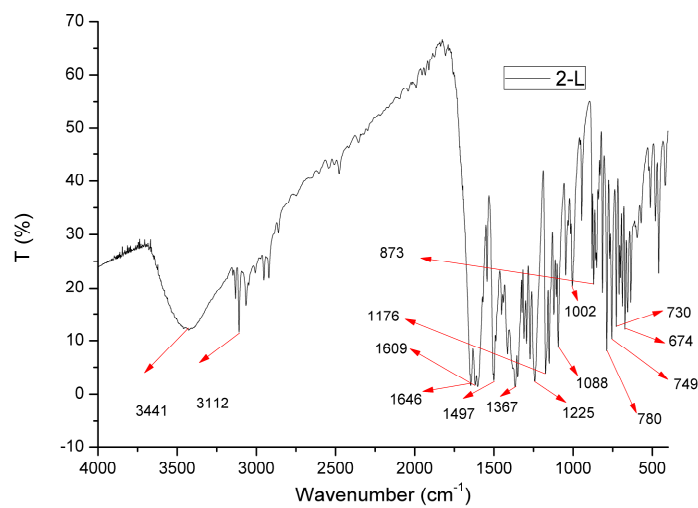
1-L					
Zn1-O4	1.958(2)	Zn1-N4a	2.057(2)	Zn1-N1	2.027(2)
Zn1-O1b	1.971(2)	O4-Zn1-N4a	93.20(10)	O4-Zn1-N1	111.57(10)
O4-Zn1-O1b	106.81(10)	N1-Zn1-N4a	107.32(9)	O1b-Zn1-N4a	119.11(11)
O1a-Zn1-N1	116.40(10)				
1-D					
Zn1-O4	1.959(2)	Zn1-N4a	2.055(2)	Zn1-N1	2.028(2)
Zn1-O1b	1.971(2)	O4-Zn1-N4a	93.20(10)	O4-Zn1-N1	111.52(10)
O4-Zn1-O1b	106.91(10)	N1-Zn1-N4a	107.39(9)	O1b-Zn1-N4a	119.00(10)
O1b-Zn1-N1	116.39(10)				
2-L					
Zn1-N1	2.010(2)	Zn1-O1a	1.935(2)	Zn1-O4	1.941(2)
Zn1-N4b	1.941(2)	N1-Zn1-N4a	103.21(9)	O1b-Zn1-N1	111.21(11)
O1b-Zn1-O4	107.84(12)	O1b-Zn1-N4a	122.00(12)	O4-Zn1-N1	118.51(10)
O4-Zn1-N4a	93.74(13)				
2-D					
Zn1-O4a	1.944(2)	Zn1-N1	2.0131(19)	Zn1-O1	1.9328(19)
Zn1-N4b	2.0388(17)	O4a-Zn1-N1	118.65(9)	O4a-Zn1-N4b	93.58(11)
N1-Zn1-N3b	103.35(8)	O1-Zn1-O4a	107.83(10)	O1-Zn1-N1	111.34(10)
O1-Zn1-N4b	121.71(10)				

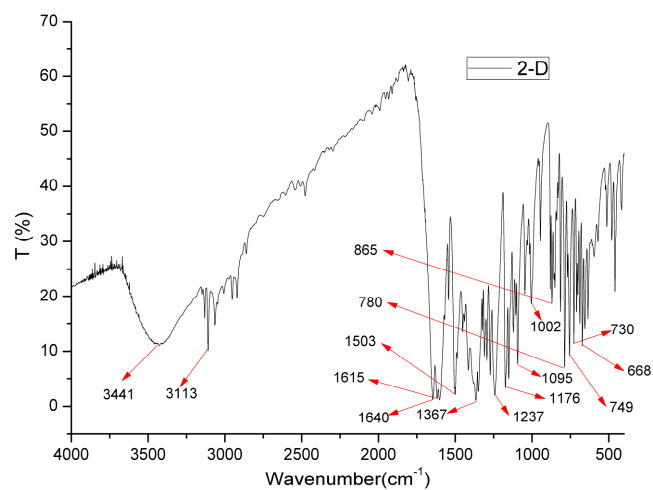
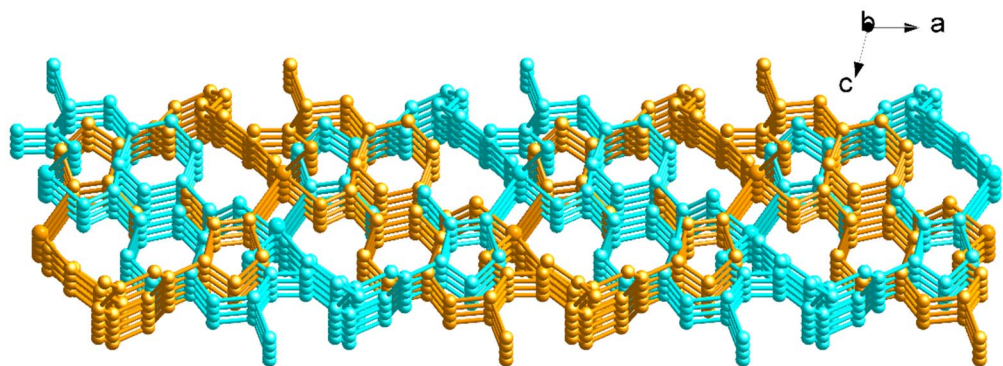
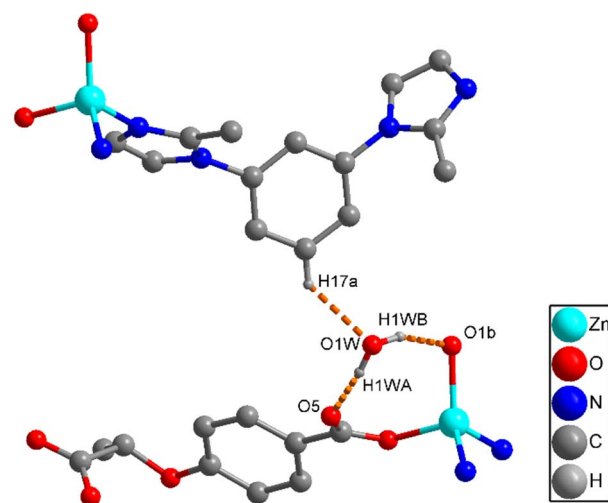
Symmetry codes: (a) $2-x, 1/2+y, 1-z$; (b) $-x, 1/2+y, 1-z$ for **1-L**; (a) $-x, -1/2+y, 1-z$; (b) $2-x, -1/2+y, 1-z$ for **1-D**; (a) $1+x, y, 1+z$; (b) $x, 1+y, z$ for **2-L**; (a) $x, 1+y, z$; (b) $-1+x, y, -1+z$ for **2-D**

Table S2. Hydrogen-bond geometry between adjacent layers in **1-L** (\AA , $^\circ$)

D—H…A	D—H	H…A	D…A	D—H…A
O1W—H1WA…O5	0.85	2.04	2.843(5)	157
O1W—H1WB…O1 ^b	0.85	2.20	2.978(5)	152
C17—H17 ^a …O1W	0.93	2.50	3.267(5)	146

Symmetry codes: (a) $1-x, 1/2+y, 2-z$; (b) $-x, 0.5+y, 1-z$

Figure S1. The IR spectra of **1-L**Figure S2. The IR spectra of **1-D**Figure S3. The IR spectra of **2-L**

Figure S4. The IR spectra of **2-D**Figure S5. 2-fold interpenetration 2D framework in **1-L**Figure S6. Hydrogen bonds between adjacent layers in **1-L**

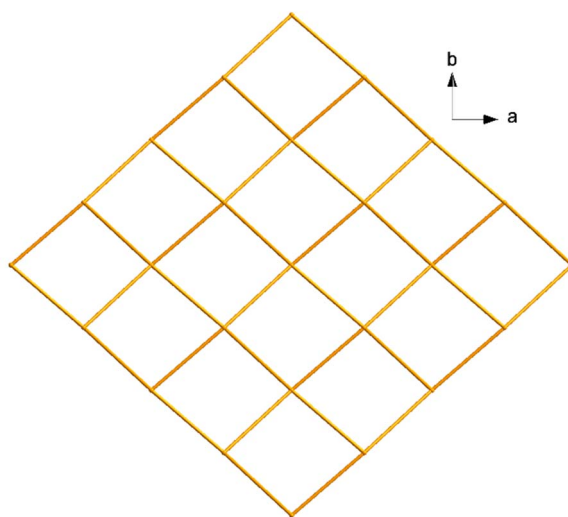


Figure S7. The sql net of compound **1-L**

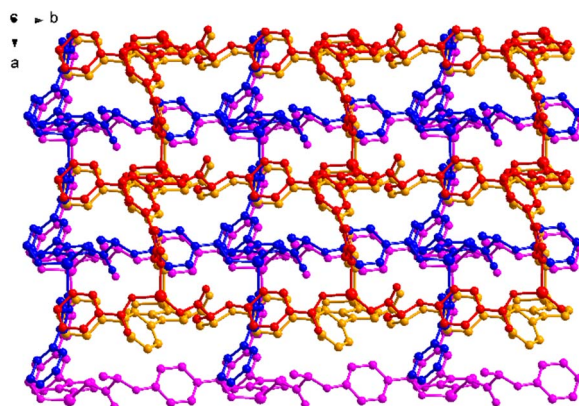


Figure S8. 4-fold interpenetration 2D framework in **2-L**

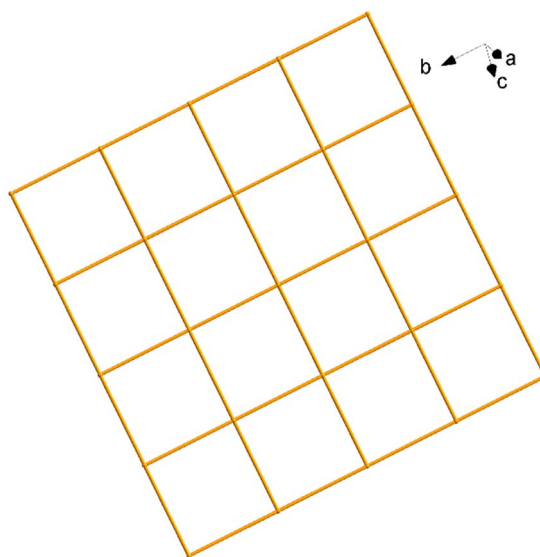


Figure S9. The sql net of compound **2-L**

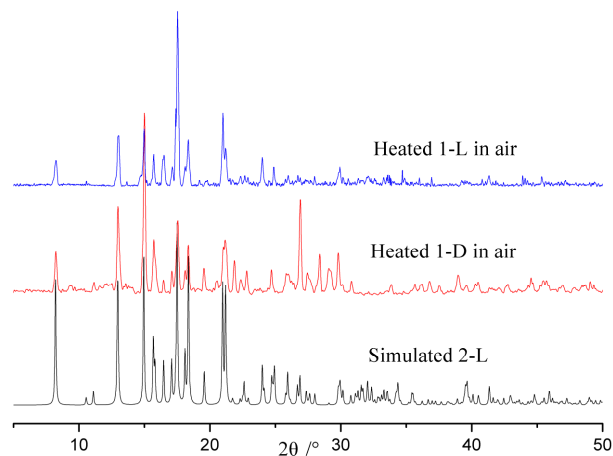


Figure S10. The PXRD patterns of heated **1-L** and **1-D** in air

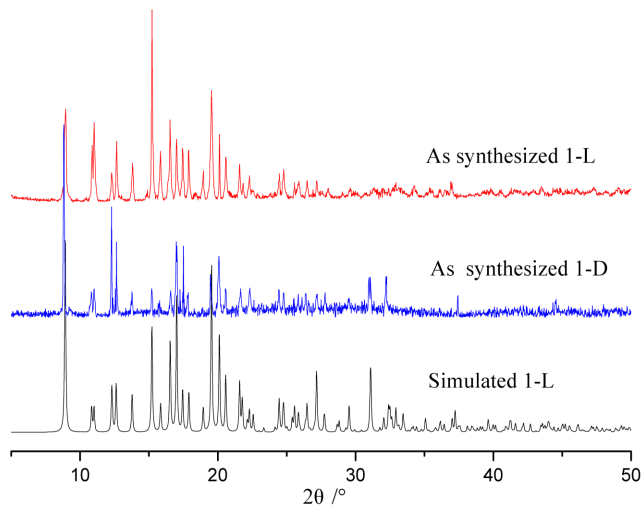


Figure S11. The PXRD patterns of **1-D** and **1-L**

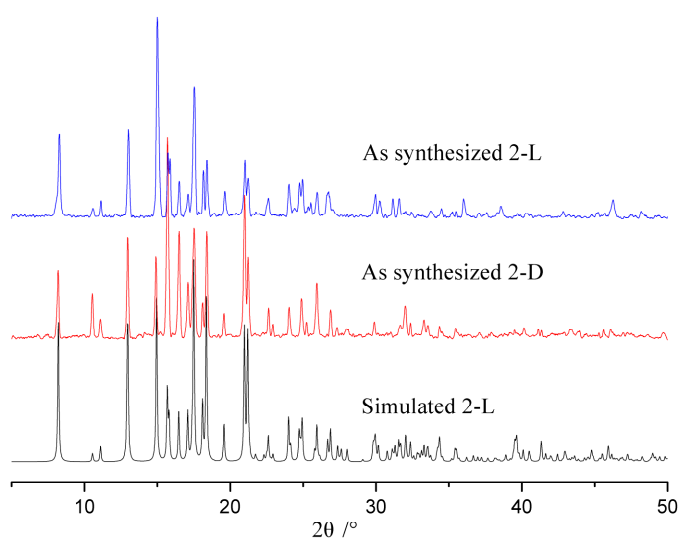
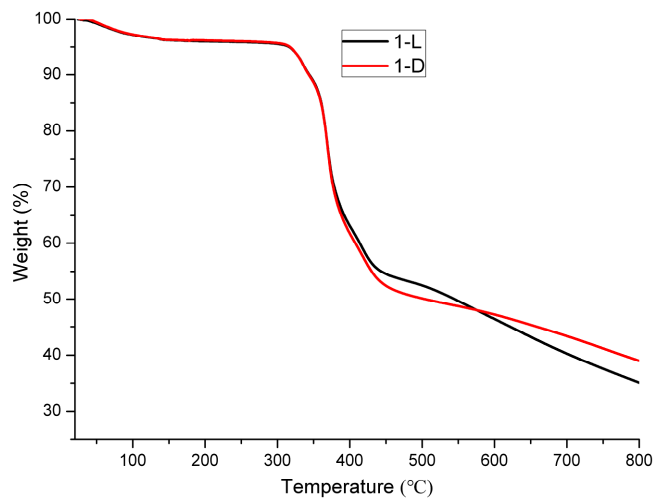
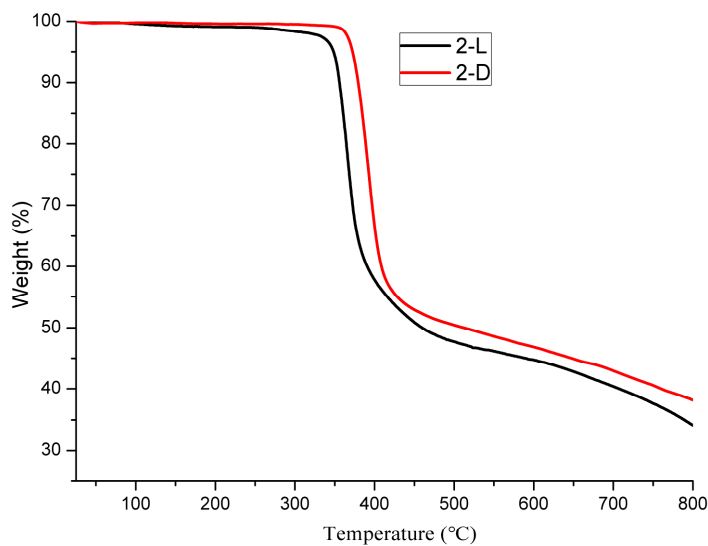


Figure S12. The PXRD patterns of **2-L** and **2-D**

Figure S13. TGA curves of **1-L** and **1-D**Figure S14. TGA curves of **2-D** and **2-L**